scientific reports

Check for updates

OPEN

Combination of morphological and multiparametric MR neurography enhances carpal tunnel syndrome diagnosis and evaluation

Youzhi Wang[1,2,5], Wenjun Wu[1,2,5], Jiamin Kang[1,3], Yu Su[1,2,5], Tingting Liu[1,2,5], Jie Zhao[1,2,5], Dingxi Liu[1,2,5], Xiangchuang Kong[1,2,5], Yuxiong Weng[4], Chuansheng Zheng[1,2,5], Chungao Li[1,2,5]✉ & Lixia Wang[1,2,5]✉

This study aimed to investigate the diagnostic and evaluative significance of combining median nerve (MN) morphological measurements with diffusion tensor imaging (DTI) and T2 mapping metrics for carpal tunnel syndrome (CTS). Morphological and multiparametric magnetic resonance neurography (MRN), along with clinical evaluation, were conducted on 33 CTS patients and 32 healthy controls. The MRN metrics included fractional anisotropy (FA), apparent diffusion coefficient (ADC), axial diffusivity (AD), radial diffusivity (RD), T2 value, cross-sectional area (CSA) and MN flattening ratio (MNFR) at both the pisiform bone and hamate bone levels. Differences in MRN metrics between the above two levels (Delta FA, Delta ADC, Delta AD, Delta RD and Delta T2) were calculated. T-tests, multivariable regression, and receiver operating characteristic (ROC) curve analyses were used to compare and classify patients with CTS and controls. The correlations between MRN metrics and clinical characteristics were analyzed. Comparisons were also made between MRN metrics in patients with and without significant symptom improvement after treatment. FA, AD, T2 value, and CSA at the pisiform bone level were identified as independent predictors of CTS. The combination of these metrics improved diagnostic performance (AUC 0.922, sensitivity 84.85% and specificity 90.62%). Delta ADC, Delta AD, and Delta T2 correlated with function Boston scores. The T2 value at hamate bone level, along with Delta AD and FA, correlated with visual analogue score (VAS). CSA and Delta T2 had higher AUCs for classifying patients with and without significant symptom improvement after treatment. These findings suggest that combining MN morphological and multiparametric MRN metrics can enhance the diagnostic performance of CTS and has the potential to provide an objective and quantitative basis for further study of the degree of entrapment and prognosis.

Keywords Carpal tunnel syndrome, Median nerve, Diffusion tensor imaging, T2 mapping

Abbreviations

CTS	Carpal tunnel syndrome
MN	Median nerve
DTI	Diffusion tensor imaging
MRN	Magnetic resonance neurography
VAS	Visual analogue score
BCTQ	Boston Carpal Tunnel Questionnaire
FA	Fractional anisotropy
ADC	Apparent diffusion coefficient
AD	Axial diffusivity
RD	Radial diffusivity

[1]Department of Radiology, Union Hospital, Tongji Medical College, Huazhong University of Science and Technology, Wuhan 430022, China. [2]Hubei Province Key Laboratory of Molecular Imaging, Jiefang Avenue #1277, Wuhan 430022, China. [3]Wuhan No. 1 Hospital, Wuhan 430033, China. [4]Department of Hand Surgery, Union Hospital, Tongji Medical College, Huazhong University of Science and Technology, Wuhan, China. [5]Hubei Provincial Clinical Research Center for Precision Radiology & Interventional Medicine, Wuhan 430022, China. ✉email: lichueng@126.com; lisa2003627_1@163.com

CSA	Cross-sectional area
MNFR	Median nerve flattening ratio

Carpal tunnel syndrome (CTS) is the most common peripheral nerve entrapment disorder, resulting in symptoms such as paraesthesia and weakness[1,2]. The preliminary evaluation for CTS is grounded in the patient's reported symptoms and physical examination findings, followed by developing a treatment plan to prevent irreversible complications, such as muscle atrophy, which can substantially impair the patient's quality of life and occupational functioning[3,4]. Although electrophysiological examinations are currently recommended for decision-making regarding treatment modalities[5], this invasive method not only has a high false positive rate but also always lacks accuracy in classifying the severity of CTS, thus failing to fully meet the requirements for preoperative evaluation[6,7]. It is imperative to incorporate imaging examinations to furnish critical anatomical information[8,9]. Nonetheless, the current management of CTS patients, encompassing both preventive measures and the assessment of treatment efficacy through imaging techniques, remains inadequate[10]. Therefore, employing a noninvasive quantitative method as an auxiliary tool for assessing the pathophysiological state of nerve in CTS is highly beneficial.

In the past decade, the utilization of magnetic resonance neurography (MRN) for evaluating peripheral nerve entrapment has emerged a significant trend, providing objective morphological insights and quantitative functional evaluations of neuropathological processes[11,12]. Morphological metrics such as routine MRI are of highly value in detecting and assessing abnormalities of the median nerve and carpal tunnel[13]. Diffusion tensor imaging (DTI) measures the diffusivity and directional properties of water molecules within tissues, quantifies microstructural characteristics, and is extensively utilized in the brain white matter[14]. DTI derived metrics, including fractional anisotropy (FA), apparent diffusion coefficient (ADC), axial diffusivity (AD), and radial diffusivity (RD), are also used to assess axon and myelin integrity, as well as to distinguish between various types of peripheral nerve injuries[15–19]. FA reflects the directionality of water diffusion, with higher values indicative of well-preserved axonal structures, whereas lower values may suggest demyelination or axonal damage. ADC quantifies overall water diffusion, with increased values suggesting tissue damage or edema and decreased values indicating cellular swelling. AD assesses diffusion parallel axons, providing insights into axon integrity. RD measures diffusion perpendicular to axons, which is particularly useful for assessing myelin integrity. T2 mapping, a technique frequently used for evaluating the microstructure of articular cartilage, has been employed to quantitatively assess neuroedema[20]. However, the effectiveness of combining these morphological and multiparametric MRN metrics for diagnosing and evaluating CTS remains to be investigated.

The objective of this study was to investigate (1) the optimal MRN metrics and the benefits of their combination for the diagnosis of CTS; and (2) the correlation between various MRN metrics and clinical severity assessments, in addition to identifying potential prognostic indicators prior to treatment. Our aim was to establish a comprehensive imaging approach for CTS and to offer additional information to support its diagnosis and management.

Materials and methods

This prospective study received approval from the institution's ethics committee (No. UHCT21809, approval date 2021-01-04). All subjects provided informed consent. All methods were performed in accordance with the relevant guidelines and regulations.

Subjects

From June 2021 to September 2022, 33 patients (27 females, 6 males) diagnosed with CTS were recruited using a convenience sampling approach. The inclusion criteria for CTS consisted of diagnoses confirmed through clinical examinations, which included a positive Tinel sign, Phalen test, paresthesia, or numbness in the area innervated by the median nerve, thumb and index finger pinching disorders, or decreased median nerve conduction velocity (NCV) in the carpal tunnel on electromyography (EMG) examination[13]. The exclusion criteria included general contraindications to MRI; a history of wrist surgery or trauma; and secondary risk factors for CTS, such as diabetes, gout, and inflammatory joint disease. 32 healthy volunteers (20 females, 12 males) with no history of clinical or neurological symptoms in the wrist were included in the control group (Table 1).

Clinical evaluation

All patients were evaluated using the visual analogue score (VAS) for pain and the Boston Carpal Tunnel Syndrome Questionnaire (BCTQ) for symptom and function. The VAS requires patients to assess their level of pain on a 10-point scale, where 0 represents no pain and 10 indicates the highest intensity of pain[21]. The BCTQ is a self-administered questionnaire that evaluates the severity of symptoms (11 questions) and functional status (8 questions) associated with CTS[22]. The duration since onset, physical signs (including the Tinel sign and Phalen test), nocturnal pain, and the sensory and strength condition of the thenar muscle were evaluated. Patients were additionally subjected to a follow-up assessment using the BCTQ three months post-treatment (either conservative or surgical) to record their prognosis.

MR image acquisition

MR imaging was conducted using a 3.0-T scanner (PHILIPS Ingenia CX, Best, Netherlands) with a dedicated 8-channel wrist coil. The MRI protocol included coronal T1-weighted imaging (T1WI), proton density-weighted imaging (PDWI), axial PDWI, DTI, and T2 mapping of the wrist. The parameters of these sequences are presented in Table 2.

General features	CTS group		Control group	
	Number	Percentage (%)	Number	Percentage (%)
Sex				
Female	27	81.81	20	62.50
Male	6	18.18	12	37.50
Position				
Left side	13	39.39	16	50.00
Right side	20	60.61	16	50.00
Age (years)	52.67 ± 5.61		48.31 ± 10.30	
Clinical evaluation				
Duration (month)	18.96 ± 22.96		0.00 ± 0.00	
Symptom Boston score	26.76 ± 5.90		1.00 ± 0.00	
Function Boston score	14.61 ± 3.56		1.00 ± 0.00	
VAS	4.76 ± 1.47		0.00 ± 0.00	

Table 1. Demographic and clinical evaluation of all subjects. *VAS* visual analogue score.

MRI sequences	TR (ms)	TE (ms)	FOV (mm^2)	Matrix	In plane resolution (mm^2)	Scan time	b value (s/mm^2)
Coronal T1WI	510	10	130 × 130	252 × 288	0.45 × 0.52	1 min	–
Coronal PDWI	2100	27	150 × 150	285 × 500	0.30 × 0.66	2 min 01 s	–
Axial PDWI	3336	27	99 × 99	260 × 396	0.25 × 0.38	2 min 20 s	–
Axial T2 mapping	3000	19	120 × 120	115 × 152	0.79 × 0.90	2 min 09 s	–
Axial DTI	2732	67	120 × 120	62 × 64	1.87 × 1.94	4 min 38 s	0 and 800

Table 2. MRI sequences and parameters. *TR* repetition time, *TE* echo time, *FOV* field of view, *T1WI* T1-weighted image, *PDWI* proton density-weighted image, *DTI* diffusion tensor imaging.

MR metric measurement and calculation

Original images were post-processed on a workstation (ISP, Philips Healthcare). Using the axial PDWI image as the anatomic reference, DTI and T2 mapping were automatically registered. The region of interest (ROI) for the median nerve was manually delineated at the levels of the pisiform and hamate bones. The values of FA, ADC, AD, RD, and T2 were measured by two radiologists (Y.W. with 5 years of experience and J.K. with 7 years of experience), and the differences between the two levels were calculated (defined as Delta FA, Delta ADC, Delta AD, Delta RD and Delta T2). For example, Delta FA is calculated using the formula: Delta FA = FA (pisiform bone level) − FA (hamate bone level). Meanwhile, the long diameter, short diameter, and cross-sectional area (CSA) were measured on the axial PDWI image at the corresponding level, and the median nerve flattening rate (MNFR) (long diameter/short diameter) was calculated. (Fig. 1).

Statistical analysis

All metrics were expressed as mean ± standard deviation (SD). The normality of the quantitative data was evaluated using the Shapiro–Wilk test. Independent sample t test (or Wilcoxon rank sum test if nonnormally distributed) was used to compare the FA, ADC, AD, RD, and T2 values, as well as the CSA and MNFR, between CTS and control groups at the pisiform and hamate bone levels. Multivariable logistic regression analysis using the forward projection method was then conducted to identify independent predictors of CTS. The model incorporated all the quantitative factors with values of $p < 0.05$ in the univariable analysis. For metrics that were found to be independent predictors in the multivariable analysis, the area under curve (AUC) was computed, and receiver operating characteristic (ROC) curves were generated. The AUC values were compared using the Delong test. Spearman coefficient was used to correlate the original and Delta MR metrics with clinical features. Patients were divided into subgroups according to the BCTQ scores before and after 3 months of follow-up, with and without significant symptoms improvement. All MR metrics were compared between the two subgroups, and ROC curve was conducted on the metrics. All statistical analyses were performed using GraphPad Prism 9.5 and Med-Calc 20.0 software, with a p value < 0.05 considered statistically significant.

Results

Comparison of MR metrics between CTS and control groups

Table 3 shows a comparison of MR metrics between the CTS and control groups. The FA, ADC, AD, RD, T2, and CSA of median nerve at the level of pisiform bone and hamate bone were significantly different between the two groups (all $p < 0.05$). FA in the CTS group was lower than that in the control group, while the other metrics were higher than those in the control group. There was no significant difference in MNFR at either level ($p > 0.05$). In multivariable stepwise logistic regression analysis of metrics with $p < 0.05$ from the univariable analysis, the

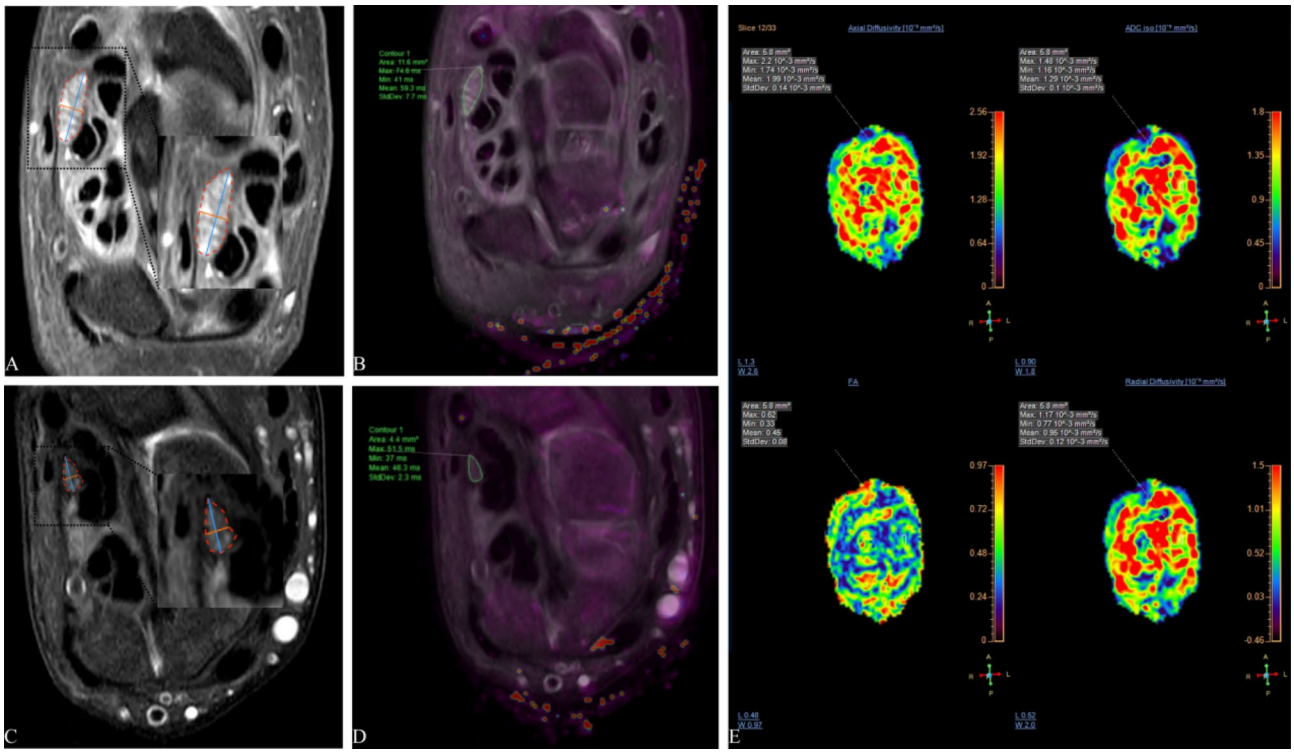

Fig. 1. Representative images illustrating the acquisition of multiple MR metrics of the median nerve at the pisiform bone level in a CTS patient (**A**,**B**) and a healthy control (**C**,**D**). The median nerve's long diameter (blue), short diameter (orange), and cross-sectional area (red) were measured on an axial PD weighted image (**A**,**C**). The median nerve's T2 values were obtained from the T2 mapping and axial PD fusion images (**B**,**D**). The median nerve's DTI metrics, including fractional anisotropy, apparent diffusion coefficient, axial diffusivity, and radial diffusivity, metrics were acquired on the color images (**E**). *PD* proton density.

Parameters	CTS (n = 33)	Control (n = 32)	p[a]	Effect size[b]	Multivariable analysis	
					Odds ratio (95% CI)	p
FA (h)	0.44 ± 0.11	0.54 ± 0.10	< 0.001**	−0.95		0.141
AD (h)	2.21 ± 0.26	2.03 ± 0.22	0.003*	0.75		0.19
ADC (h)	1.44 ± 0.18	1.22 ± 0.21	< 0.001**	1.12		0.924
RD (h)	1.05 ± 0.21	0.82 ± 0.25	< 0.001**	1.00		0.433
T2 (h)	60.81 ± 9.13	53.43 ± 6.71	< 0.001**	0.92		0.567
MNFR (h)	2.40 ± 0.63	2.27 ± 0.78	0.479	0.18		
CSA (h)	12.32 ± 7.71	9.25 ± 2.46	0.036*	0.53		0.33
FA (p)	0.43 ± 0.11	0.53 ± 0.13	0.001*	−0.83	< 0.001 (< 0.001–0.226)	0.045*
AD (p)	2.20 ± 0.27	2.02 ± 0.22	0.004*	0.73	4.148 (2.491–6.908)	0.039*
ADC (p)	1.46 ± 0.13	1.25 ± 0.23	< 0.001**	1.12		0.896
RD (p)	1.09 ± 0.16	0.84 ± 0.24	< 0.001**	−0.78		0.167
T2 (p)	62.07 ± 8.49	54.50 ± 8.44	< 0.001**	0.89	1.321 (1.048–1.664)	0.018*
MNFR (p)	2.33 ± 0.57	2.18 ± 0.46	0.27	0.29		
CSA (p)	14.23 ± 5.89	9.49 ± 2.68	< 0.001	1.04	1.543 (1.052–2.263)	0.026*

Table 3. Comparison of MR metrics at different levels between CTS and control group. All data are presented as mean ± SD, [a] From univariable analyses, [b]Cohen's d value,*p < 0.05, **p < 0.001. *CSA* cross-sectional area, *CTS* carpal tunnel syndrome, *FA* fractional anisotropy, *AD* axial diffusivity, *ADC* apparent diffusion coefficient, *RD* radial diffusivity, *CSA* cross-sectional area, *MNFR* flattening ratio of the median nerve, *RD* radial diffusivity, *(p)* at the pisiform bone level, *(h)* at the hamate bone level.

independent predictors were identified as FA (odds ratio [OR], < 0.001; 95% CI, < 0.001–0.226; p = 0.045), AD (OR, 4.148; 95% CI, 2.491–6.908; p = 0.039), T2 value (OR, 1.321; 95% CI, 1.048–1.664; p = 0.018) and CSA (OR, 1.543; 95% CI, 1.052–2.263; p = 0.026) at the pisiform bone level. Figure 2 shows box plots of the four identified independent predictors comparing CTS to controls.

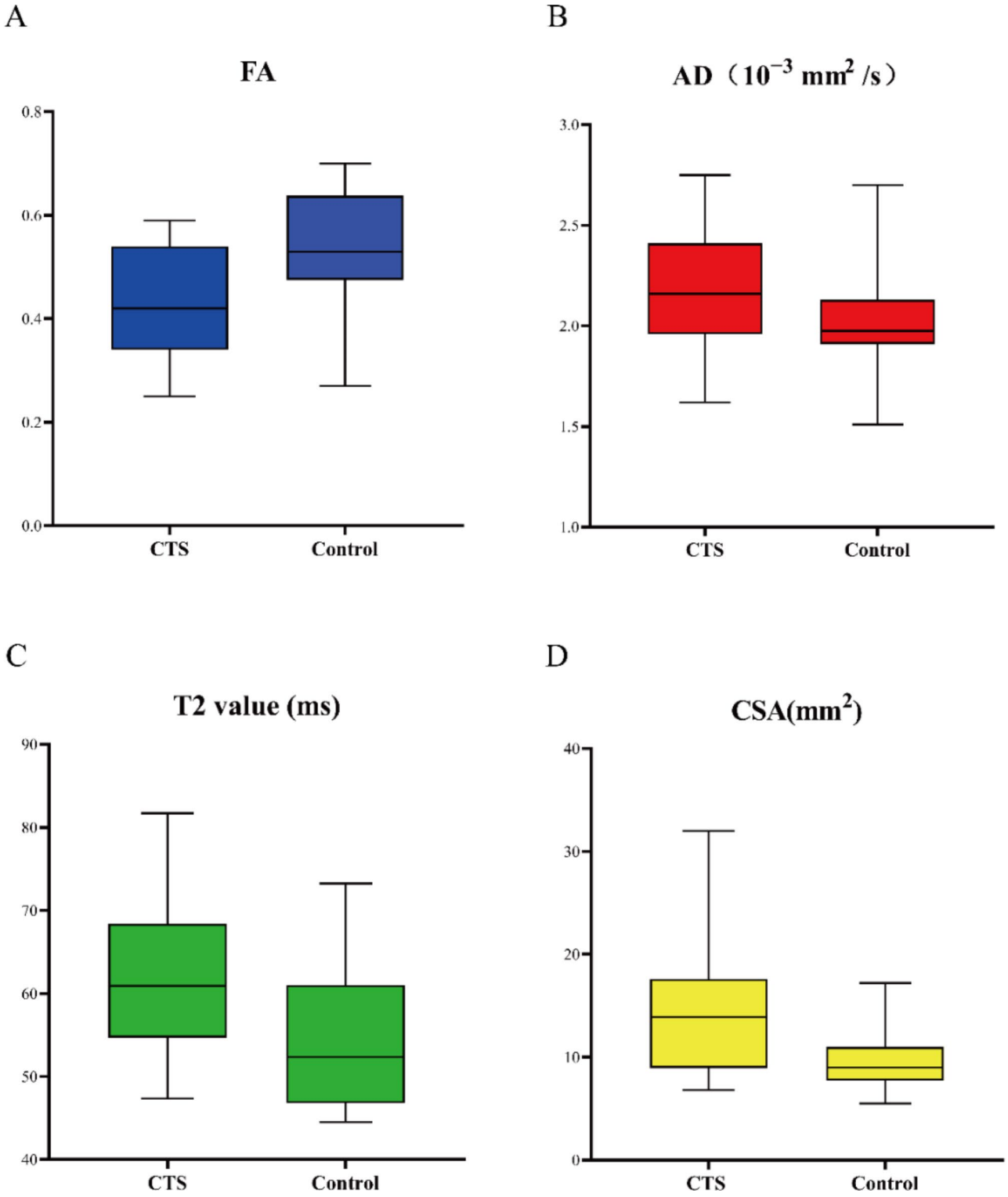

Fig. 2. Box plots comparing CTS and controls in terms of four independent predictors identified by multivariate analysis. Plots show fractional anisotropy (FA) (**A**), axial diffusivity (AD) (**B**), T2 value (**C**), and cross-sectional area (CSA) (**D**) measured at the pisiform bone level.

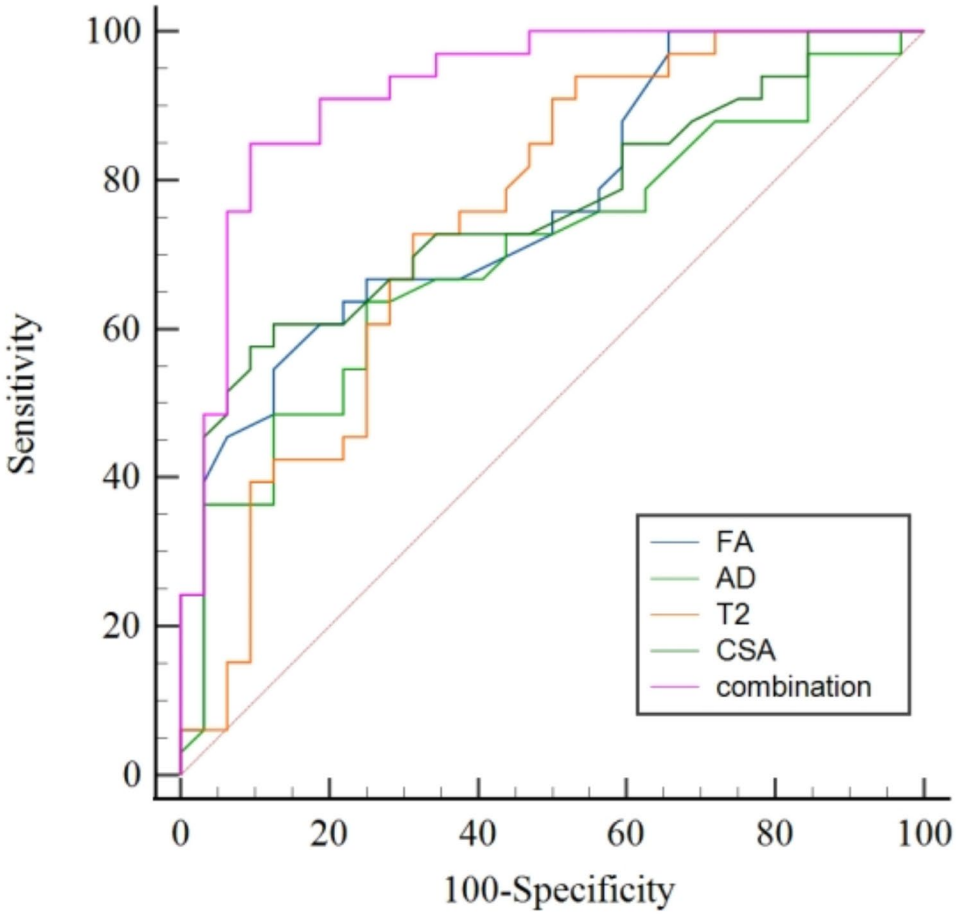

Fig. 3. The ROC curves of MR metrics for diagnosing carpal tunnel syndrome. *FA* fractional anisotropy, *AD* axial diffusivity, *CSA* cross-sectional area.

Parameters	Cutoff value	Sensitivity (95% CI)	Specificity (95% CI)
FA	< 0.42	54.55% (36.4–71.9)	87.50% (71.0–96.5)
AD	> 2.07	63.64% (45.1–79.6)	75.00% (56.6–88.5)
T2 value	> 56.35	72.73% (54.5–86.7)	68.75% (50.0–83.9)
CSA	> 12.90	57.58% (39.2–74.5)	90.62% (75.0–98)
Combination	> 0.58	84.85% (68.1–94.9)	90.62% (75.0–98)

Table 4. The diagnostic performance of MR metrics for CTS. All data at the pisiform bone level. *FA* fractional anisotropy, *AD* axial diffusivity, *CSA* cross-sectional area.

Diagnostic performance of MR metrics

The AUCs for the four identified independent predictors of CTS, all measured at the pisiform bone level, were 0.764 (95% CI, 0.642–0.860) for FA, 0.701 (95% CI, 0.573–0.830) for AD, 0.747 (95% CI, 0.626–0.644) for T2 value, and 0.761 (95% CI, 0.644–0.879) for CSA. The AUC for the combination of these four metrics was 0.922 (95% CI, 0.856–0.989). The AUC of the multi-metrics combination was significantly greater than that of individual metric (all $p < 0.05$). Figure 3 displays the ROC curves for the combined and individual metrics. Table 4 shows the derived optimal thresholds of the metrics, along with their sensitivity and specificity in diagnosing CTS.

Correlations between MR metrics and clinical evaluation

Figure 4 illustrates the correlations between DTI metrics, T2 values, Delta metrics (including Delta FA, Delta ADC, Delta AD, Delta RD, and Delta T2), morphological metrics (including CSA and MNFR) and clinical evaluations in CTS patients. Delta AD and Delta ADC exhibited a positive correlation with BCTQ functional scores, while Delta T2 showed a negative correlation with functional scores. T2 value at the hamate bone level and Delta AD were positively correlated with VAS, whereas FA at the hamate bone level was negatively correlated with VAS.

Comparison of pre-treatment MR metrics between CTS patients with and without significant symptoms improvement

Electronic medical records were reviewed to classify these patients into two groups: CTS patients with (n = 7) and without (n = 9) significant symptoms improvement at the 3-month follow-up after treatment on basis of pain assessment and improvement in functional recovery before and after treatment[23]. The ROC analysis of multiple MR metrics revealed that the AUCs of CSA and Delta T2 were superior to those of others in distinguishing between the two groups. CSA at the hamate bone level showing the highest AUC (0.786 [95% CI, 0.514–0.946] vs. CSA at the pisiform bone level, with AUC of 0.754 [95% CI, 0.480–0.930] vs. Delta T2, with AUC of 0.730 [95% CI, 0.456–0.916]). The DTI metrics demonstrated little distinguishing ability. Table 5 lists the MR metrics and corresponding AUCs for the subgroups with and without significant symptoms improvement, and Fig. 5 shows the ROC curves of the metrics with the top three AUCs.

Discussion

This study comprehensively investigated the diagnostic and evaluative value of morphological and multiparametric MRN-derived metrics, both individually and in combination. FA, AD, T2 value, and CSA at the pisiform bone level were identified as independent predictors of CTS through multivariable regression analysis, with their combination demonstrating superior diagnostic performance compared with each metrics alone. DTI and T2 mapping-derived metrics were strongly correlated with functional and pain evaluations and could be used to monitor the severity of CTS. The CSA and Delta T2 might be potential indicators of prognosis.

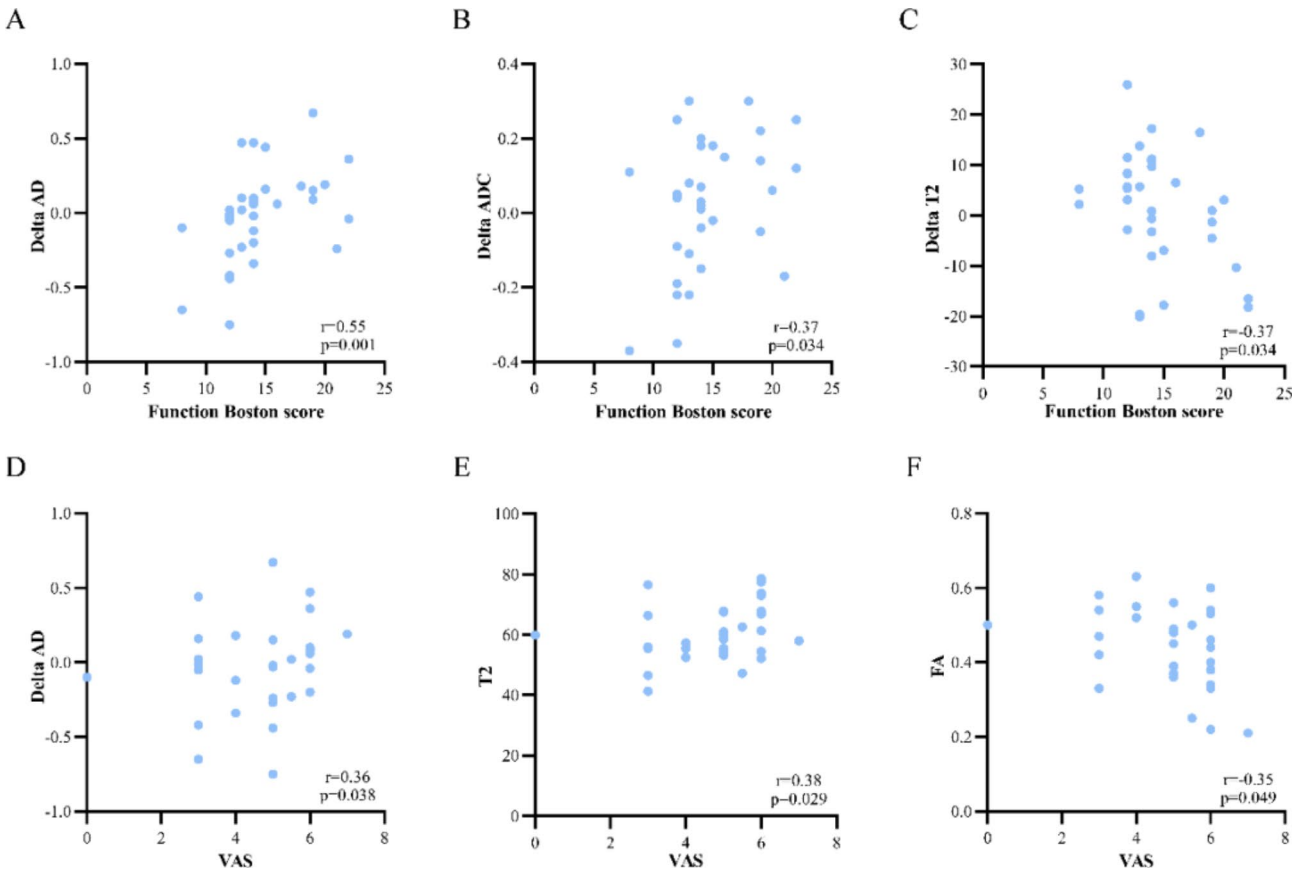

Fig. 4. Scatterplots of correlations between MR metrics and clinical characteristics. Plots show the correlations between Delta AD (**A**), Delta ADC (**B**), Delta T2 (**C**), and Function Boston score, and the correlations between FA, T2 at the hamate bone level, Delta AD and VAS. "Delta" is calculated by subtracting the measurement at the hamate level from that at the pisiform level. *FA* fractional anisotropy, *ADC* apparent diffusion coefficient, *AD* axial diffusivity, *VAS* visual analogue score.

	Without significant symptoms improvement (n = 7)	With significant symptoms improvement (n = 9)	AUC	95%CI
FA (h)	0.48 ± 0.05	0.41 ± 0.16	0.603	0.335–0.833
AD (h)	2.22 ± 0.27	2.17 ± 0.26	0.579	0.313–0.815
ADC (h)	1.37 ± 0.19	1.44 ± 0.18	0.698	0.424–0.897
RD (h)	0.98 ± 0.15	1.10 ± 0.26	0.619	0.349–0.844
T2 (h)	55.55 ± 9.86	59.42 ± 6.06	0.619	0.349–0.844
MNFR (h)	2.58 ± 0.65	2.52 ± 0.79	0.587	0.320–0.821
CSA (h)	10.61 ± 4.23	18.93 ± 11.82	0.786	0.514–0.946
FA (p)	0.44 ± 0.09	0.40 ± 0.12	0.659	0.386–0.871
AD (p)	2.17 ± 0.30	2.10 ± 0.15	0.579	0.313–0.815
ADC (p)	1.42 ± 0.12	1.45 ± 0.15	0.540	0.279–0.785
RD (p)	1.05 ± 0.11	1.11 ± 0.20	0.651	0.378–0.866
T2 (p)	63.82 ± 10.62	59.42 ± 6.06	0.571	0.307–0.809
MNFR (p)	2.21 ± 0.54	2.44 ± 0.51	0.667	0.393–0.876
CSA (p)	11.56 ± 3.39	18.02 ± 6.77	0.754	0.480–0.930
Delta FA	0.01 ± 0.11	− 0.02 ± 0.08	0.540	0.279–0.785
Delta AD	0.05 ± 0.13	0.01 ± 0.16	0.507	0.253–0.760
Delta ADC	− 0.04 ± 0.17	− 0.07 ± 0.23	0.603	0.335–0.833
Delta RD	0.07 ± 0.19	0.01 ± 0.18	0.571	0.307–0.809
Delta T2	8.27 ± 9.36	1.35 ± 8.67	0.730	0.456–0.916

Table 5. Comparison of MR metrics between patients with and without significant symptoms improvement. *FA* fractional anisotropy, *AD* axial diffusivity, *ADC* apparent diffusion coefficient, *RD* radial diffusivity, *CSA* cross-sectional area, *MNFR* flattening ratio of the median nerve, *(p)* at the pisiform bone level, *(h)* at the hamate bone level. "Delta" represented the differences of metrics between the hamate bone and the pisiform bone levels.

Morphological assessment of the median nerve has long been used to detect CTS[13,24]. Among these measurements, the diagnostic efficacy of CSA for CTS has been well-established among the various measurements[24]. We also found that the CSA of the median nerve was enlarged in CTS patients, especially at the pisiform bone level, corresponding to the nerve swelling location at the carpal tunnel entrance as reported by Koh et al.[25]. However, our study showed no significant difference in the MNFR between CTS and control groups. Currently, the diagnostic efficacy of the MNFR for CTS remains controversial. Ng et al. observed a significant elevation of MNFR significantly at the carpal tunnel entrance in CTS patients compared to healthy controls, attributed to a flattened nerve entrapment[24]. Vo et al. reported significant differences in MNFR at the hamate level; however, they concluded that MNFR was less effective than CSA for diagnosing and grading CTS[26]. The ultrasound findings by Chang et al. and Roll et al. did not reveal any notable difference in MNFR[27,28]. We hypothesized that the anatomical deformations and nerve swelling, induced by varying degrees of nerve compression, would lead to less pronounced alterations in MNFR compared to CSA in CTS patients.

In the past two decades, DTI has become a valuable tool to evaluate the integrity of peripheral nerves[12]. Decreased FA and increased ADC are the major findings in peripheral neuropathies, including CTS, reflecting enhanced water diffusion, reduced anisotropy, and disruption of restricted structure due to nerve damage[15,16,29–31]. FA and ADC at the pisiform bone level or the most swollen site had the highest diagnostic values[18,29], with the FA's performance surpassing that of ADC, which is consistent with our findings[25]. With respect to AD and RD, Vo et al. observed increased RD in CTS but no significant difference in AD[16]. Wu et al. found that increased AD in patients with chronic inflammatory demyelinating polyradiculoneuropathy, which was attributed to axonal degeneration and endoneurial edema[32]. In this study, both RD and AD were increased in CTS, with AD serving as a predictor for distinguishing CTS from controls. Pathophysiologically, the mechanisms of CTS include microcirculation impairment, axonal degeneration, demyelination, and inflammatory changes caused by entrapment and traction[33]. Therefore, we speculate that AD in CTS is influenced by comprehensive pathological factors and can be used as a diagnostic indicator of CTS, but further verification is needed.

Additionally, we applied T2 mapping of the median nerve to differentiate CTS from controls, which has been less studied. Maeda et al. found significantly increased T2 values of the median nerve proximal to the carpal tunnel in CTS patients, with an average of 56.7 ms[34]. A 7 T MRI study showed that the mean T2 value of median nerve in CTS was 24.27 ms, significantly higher than in healthy volunteers[35]. Similarly, our study showed that the optimal cut-off threshold for T2 value at the pisiform bone level was 56.35 ms. Moreover, T2 value demonstrated predictive value in distinguishing CTS from controls in this study. Bruno et al. found that the T2 value of the compressed nerve root increased significantly in lumbar disc herniation was related to nerve edema, suggesting active inflammation[20]. Therefore, we believe that the combination of FA, AD, T2 value and CSA offers superior diagnostic performance than the individual metrics do because of its comprehensive depiction of nerve integrity, neuroedema and morphological enlargement of the median nerve.

Through the correlation analysis between MR metrics and clinical evaluation, we found that Delta AD and Delta ADC were associated with BCTQ functional scores, while FA at the hamate bone level and Delta AD was

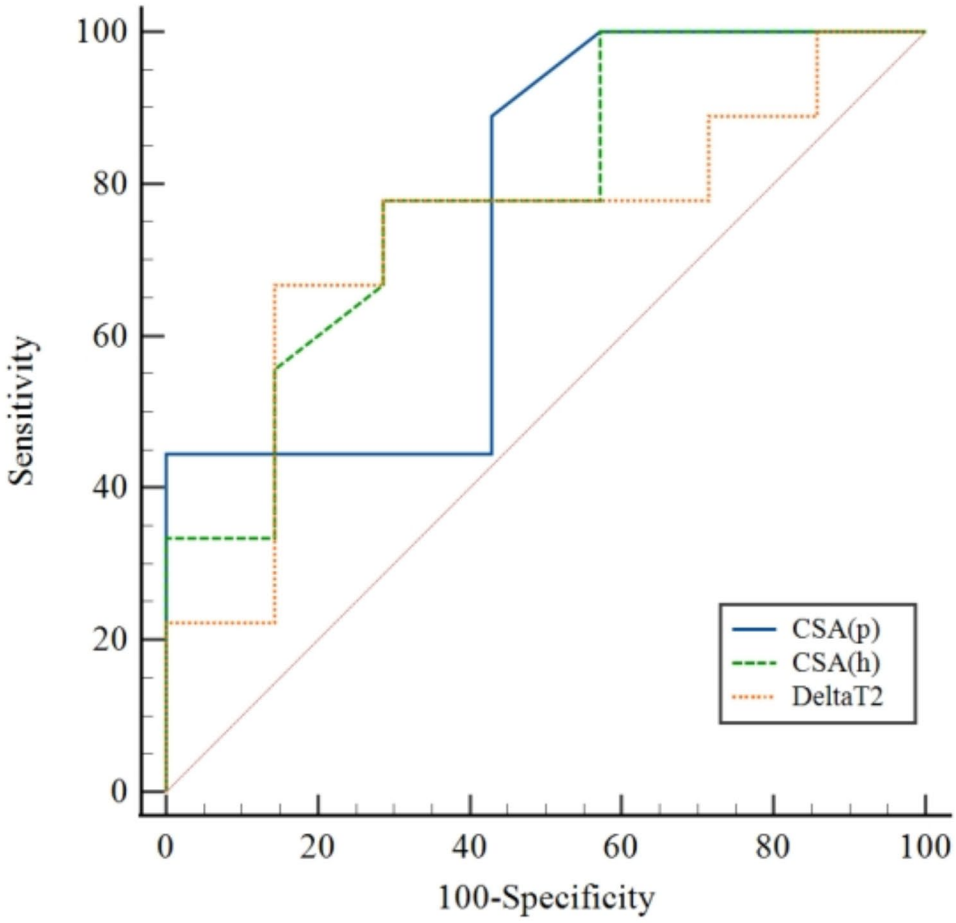

Fig. 5. The ROC curves of CSA and Delta T2 value for predicting the prognosis of carpal tunnel syndrome. *CSA*, cross-sectional area; *(p)* at the pisiform bone level; *(h)* at the hamate bone level.

associated with VAS. A previous study also showed that Delta FA and Delta ADC positively correlated with distal motor latency time[16]. This may be due to the chronic entrapment of the median nerve and distal Wallerian degeneration, which affects the electrical activity of the nerve[36]. Wu et al. found that FA was related to axon density and myelin thickness, and ADC was correlated with nerve swelling and limb function in the rabbit sciatic nerve chronic constriction model[37], suggesting the potential of DTI metrics in grading CTS severity. In previous studies, no significant correlation was found between T2 and the severity of CTS or the degree of median nerve swelling[34,38]. The increase in T2 values primarily indicates elevated nerve water content due to vasogenic edema, or even a reduction in water content due to neurofibrosis as the disease progresses[20]. Our study revealed a significant correlation between Delta T2 and functional scores, as well as between T2 value and VAS, highlighting the valuable role of T2 mapping in the evaluation of CTS.

The quantitative MRN metrics of median nerve morphology and function offer objective parameter thresholds for identifying CTS patients, providing insights into current neuropathological conditions. For instance, FA indicates myelin damage and T2 reflects the degree of nerve swelling after nerve entrapment, thereby significantly enhancing diagnostic confidence. Furthermore, establishing standardized criteria for assessing clinical severity will aid in selecting appropriate treatment options, whether conservative or surgical. These quantitative indicators will support the development of such standards. Furthermore, in comparison to the subjective nature of clinical assessments and the invasive procedures of electrophysiological testing, the noninvasive and reproducible characteristics of MRN are more advantageous monitoring post-treatment changes in CTS. It allows for dynamic evaluation of the therapeutic outcomes, and facilitates timely adjustments to treatment plans.

We sought to elucidate whether pre-treatment DTI metrics, T2 value, CSA and Delta metrics of the median nerve could distinguish CTS patients with and without significant symptom improvement after treatment. It was found that CSA at both levels and Delta T2 were the only three metrics with AUC > 0.7, and the AUCs of other metrics were all > 0.5. Wu et al. detected changes in CSA before and after carpal tunnel release using ultrasound, finding CSA significantly correlated with the severity, yet no significant changes occurred after surgery due to

delayed postoperative decompression[39]. Delta T2 can be used as a supplementary metric for nerve swelling in prognostic determinations. Pridmore et al. utilized DTI to track median nerve or ulnar nerve injury at different intervals post-repair and discovered that an increase in FA indicated nerve repair and regeneration[40]. Kim et al. evaluated the prognosis of ulnar neuropathy at the elbow using preoperative DTI, showing that FA had the strongest association with clinical outcomes and was influenced by different measurement levels[23]. Although DTI metrics were not the strongest determinants in this study, they still offered some clues for identifying CTS patients with potentially better clinical outcomes. Patients with poorer pre-treatment imaging results generally had significant symptoms improvement after treatment, indicating that CTS should not be overtreated.

We acknowledge that this study has several limitations. Firstly, the sample size was limited, and given the rising incidence of CTS among younger individuals, a more extensive age range and a balanced gender distribution of participants are required to ensure the applicability of findings to diverse population cohorts. To elucidate the impact of age and gender distribution on our findings, we conducted an analysis of MR metrics' differences across various age groups and genders, encompassing both healthy individuals and patients. Among healthy volunteers, older adults exhibited reduced FA and increased ADC and RD at the hamate level, which is consistent with findings by Guggenberger et al. and Kronlage et al., indicating age-related nerve fiber loss and demyelination[31,41]. In contrast, elderly CTS patients demonstrated a decrease in CSA and an increase in AD, with no significant changes in FA or ADC. Similarly, Moschovos et al. reported smaller CSA values in elderly patients, suggesting axonal loss, with AD closely linked to axonal damage[42]. These findings highlight the necessity for further investigation to delineate the severity of the condition across different age groups. Additionally, we observed a sex imbalance among CTS patients in our study, which is consistent with the gender distribution of CTS[1]. However, this imbalance was not present in the healthy control group and should be noted, despite previous studies suggesting that sex does not systematically influence DTI metrics[31,41]. Secondly, the clinical evaluation was solely based on typical symptoms and physical examination. A more precise severity grading system for CTS patients is needed to uncover more potential links. Thirdly, the limited short follow-up period constrained our ability to thoroughly evaluate long-term outcomes. Additionally, although our analysis facilitated a clinical evaluation of post-treatment changes relatives to pre-treatment MR metrics, the lack of longitudinal data at multiple time points post-treatment impeded a comprehensive understanding of dynamic changes over time. Future studies that monitor changes in MR metrics will provide more evidence to predict prognosis.

Conclusion

The combination of CSA, DTI metrics and T2 value of the median nerve demonstrates superior diagnostic performance for CTS than individual metrics. Multiple MR metrics are correlated well with BCTQ functional scores and VAS, suggesting their potential in grading CTS severity. Pre-treatment MR metrics also held promise in predicting prognosis. In summary, the integration of morphological and multiparametric MRN not only improves the diagnostic accuracy but also provides insights into disease severity and prognosis, offering potential guidance for personalized patient management.

Data availability

The datasets used and/or analyzed during the current study are available from the corresponding author on reasonable request.

Received: 15 July 2024; Accepted: 24 December 2024
Published online: 02 January 2025

References

1. Padua, L. et al. Carpal tunnel syndrome: updated evidence and new questions. *Lancet Neurol.* **22**, 255–267 (2023).
2. Manoharan, D., Sudhakaran, D., Goyal, A., Srivastava, D. N. & Ansari, M. T. Clinico-radiological review of peripheral entrapment neuropathies—Part 1 upper limb. *Eur. J. Radiol.* **131**, 109234 (2020).
3. Genova, A., Dix, O., Saefan, A., Thakur, M. & Hassan, A. Carpal tunnel syndrome: a review of literature. *Cureus* https://doi.org/10.7759/cureus.7333 (2020).
4. Chammas, M. et al. Carpal tunnel syndrome—Part I (anatomy, physiology, etiology and diagnosis). *Rev. Bras. Ortop. Engl. Ed.* **49**, 429–436 (2014).
5. Chong, H., See, A., Kulkarni, K., ELECTS Collaborators. National trends in the initial diagnosis and management of carpal tunnel syndrome: results from the ELECTS (ELEctrophysiology in Carpal Tunnel Syndrome) study. *Ann. R. Coll. Surg. Engl.* **106**, 64–69 (2024).
6. Graham, B. The value added by electrodiagnostic testing in the diagnosis of carpal tunnel syndrome. *J. Bone Joint Surg. Am.* **90**, 2587–2593 (2008).
7. Sasaki, T. et al. Evaluation of the existing electrophysiological severity classifications in carpal tunnel syndrome. *J. Clin. Med.* **11**, 1685 (2022).
8. Sergeant, A.-C. et al. Carpal tunnel ultrasound: is the 'safe zone' on the ulnar side of the median nerve really avascular?. *Eur. Radiol.* **30**, 887–894 (2020).
9. Warburton, C. et al. Identifying anatomic landmarks and median nerve characteristics for the analysis of persistent carpal tunnel syndrome using magnetic resonance imaging (MRI). *Skeletal Radiol.* **53**, 299–305 (2024).
10. Dahlin, L. B. et al. Carpal tunnel syndrome. *Nat. Rev. Dis. Primer* **10**, 37 (2024).
11. Sneag, D. B. & Queler, S. Technological advancements in magnetic resonance neurography. *Curr. Neurol. Neurosci. Rep.* **19**, 75 (2019).
12. Martín Noguerol, T. et al. Functional MR neurography in evaluation of peripheral nerve trauma and postsurgical assessment. *RadioGraphics* **39**, 427–446 (2019).
13. Funahashi, T. et al. Visualization of the morphological changes in the median nerve after carpal tunnel release using three-dimensional magnetic resonance imaging. *Eur. Radiol.* **32**, 3016–3023 (2022).

14. Tae, W.-S., Ham, B.-J., Pyun, S.-B., Kang, S.-H. & Kim, B.-J. Current clinical applications of diffusion-tensor imaging in neurological disorders. *J. Clin. Neurol.* **14**, 129 (2018).
15. Khalil, C. et al. Diffusion tensor imaging and tractography of the median nerve in carpal tunnel syndrome: preliminary results. *Eur. Radiol.* **18**, 2283–2291 (2008).
16. Vo, N. Q. et al. Quantitative parameters of diffusion tensor imaging in the evaluation of carpal tunnel syndrome. *Quant. Imaging Med. Surg.* **12**, 3379–3390 (2022).
17. Rojoa, D., Raheman, F., Rassam, J. & Wade, R. G. Meta-analysis of the normal diffusion tensor imaging values of the median nerve and how they change in carpal tunnel syndrome. *Sci. Rep.* **11**, 20935 (2021).
18. Liu, C. et al. Optimal parameters and location for diffusion tensor imaging in the diagnosis of carpal tunnel syndrome: a meta-analysis. *Clin. Radiol.* **73**(1058), e11-1058.e19 (2018).
19. Heckel, A. et al. Peripheral nerve diffusion tensor imaging: assessment of axon and myelin sheath integrity. *PLoS One* **10**, e0130833 (2015).
20. Bruno, F. et al. Advanced MRI imaging of nerve roots in lumbar radiculopathy due to discoradicular conflict: DWI, DTI, and T2 mapping with clinical and neurophysiological correlations. *Radiol. Med. (Torino)* **127**, 1270–1276 (2022).
21. Choinière, M. & Amsel, R. A visual analogue thermometer for measuring pain intensity. *J. Pain Symptom Manag.* **11**, 299–311 (1996).
22. Trybus, M., Koziej, M., Belka, M., Bednarek, M. & Banach, M. The Polish version of the Boston Carpal Tunnel Questionnaire: Associations between patient-rated outcome measures and nerve conduction studies. *J. Plast. Reconstr. Aesthet. Surg.* **72**, 924–932 (2019).
23. Kim, K. H. et al. Ulnar neuropathy at the elbow: associations of pre-operative DTI parameters with clinical outcomes after cubital tunnel decompression. *Eur. Radiol.* **33**, 6351–6358 (2023).
24. Ng, A. W. H. et al. MRI criteria for diagnosis and predicting severity of carpal tunnel syndrome. *Skeletal Radiol.* **49**, 397–405 (2020).
25. Koh, S. H. et al. A comparison of the performance of anatomical MRI and DTI in diagnosing carpal tunnel syndrome. *Eur. J. Radiol.* **83**, 2065–2073 (2014).
26. Vo, N. Q. et al. Magnetic resonance imaging as a first-choice imaging modality in carpal tunnel syndrome: new evidence. *Acta Radiol. Stockh. Swed.* **1987**(64), 675–683 (2023).
27. Chang, Y.-W. et al. Ratio and difference of the cross-sectional area of median nerve to ulnar nerve in diagnosing carpal tunnel syndrome: a case control study. *BMC Med. Imaging* **19**, 52 (2019).
28. Roll, S. C., Evans, K. D., Li, X., Freimer, M. & Sommerich, C. M. Screening for carpal tunnel syndrome using sonography. *J. Ultrasound Med. Off. J. Am. Inst. Ultrasound Med.* **30**, 1657–1667 (2011).
29. Klauser, A. S. et al. Carpal tunnel syndrome assessment with diffusion tensor imaging: Value of fractional anisotropy and apparent diffusion coefficient. *Eur. Radiol.* **28**, 1111–1117 (2018).
30. Razek, A. A. K. A., Shabana, A. A. E., El Saied, T. O. & Alrefey, N. Diffusion tensor imaging of mild-moderate carpal tunnel syndrome: correlation with nerve conduction study and clinical tests. *Clin. Rheumatol.* **36**, 2319–2324 (2017).
31. Guggenberger, R. et al. Assessment of median nerve with MR neurography by using diffusion-tensor imaging: normative and pathologic diffusion values. *Radiology* **265**, 194–203 (2012).
32. Wu, F. et al. Microstructural alteration of lumbosacral nerve roots in chronic inflammatory demyelinating polyradiculoneuropathy: insights from DTI and correlations with electrophysiological parameters. *Acad. Radiol.* **29**, S175–S182 (2022).
33. Aboonq, M. S. Pathophysiology of carpal tunnel syndrome. *Carpal Tunn. Syndr.*
34. Maeda, A. et al. T2 mapping of the median nerve in patients with carpal tunnel syndrome and healthy volunteers. *Muscle Nerve* **63**, 774–777 (2021).
35. Riegler, G. et al. High-resolution axonal bundle (fascicle) assessment and triple-echo steady-state T2 mapping of the median nerve at 7 T: Preliminary experience. *Investig. Radiol.* **51**, 529–535 (2016).
36. Chaudhry, V. & Cornblath, D. R. Wallerian degeneration in human nerves: Serial electrophysiological studies. *Muscle Nerve* **15**, 687–693 (1992).
37. Wu, W. et al. Application of diffusion tensor imaging in quantitatively monitoring chronic constriction injury of rabbit sciatic nerves: correlation with histological and functional changes. *Br. J. Radiol.* https://doi.org/10.1259/bjr.20170414 (2017).
38. Cha, J. G., Han, J. K., Im, S. B. & Kang, S. J. Median nerve T2 assessment in the wrist joints: Preliminary study in patients with carpal tunnel syndrome and healthy volunteers. *J. Magn. Reson. Imaging* **40**, 789–795 (2014).
39. Wu, H. et al. Ultrasound and elastography role in pre- and post-operative evaluation of median neuropathy in patients with carpal tunnel syndrome. *Front. Neurol.* **13**, 1079737 (2022).
40. Pridmore, M. D. et al. Initial findings in traumatic peripheral nerve injury and repair with diffusion tensor imaging. *Ann. Clin. Transl. Neurol.* **8**, 332–347 (2021).
41. Kronlage, M. et al. Peripheral nerve diffusion tensor imaging (DTI): normal values and demographic determinants in a cohort of 60 healthy individuals. *Eur. Radiol.* **28**, 1801–1808 (2018).
42. Moschovos, C. et al. The diagnostic accuracy of high-resolution ultrasound in screening for carpal tunnel syndrome and grading its severity is moderated by age. *Clin. Neurophysiol.* **130**, 321–330 (2019).

Author contributions

YW performed the literature search and drafted and critically revised the work. YS and TL collected analyzed the patient clinical data. WW and JK provided statistical advice and active guidance in interpreting statistical results. JZ, DL, and XK provided radiological measurements, technique, and interpretation. YW and CZ provided software support. CL and LW supervised the entire process. All authors contributed to the writing of the manuscript and read and approved the final manuscript.

Funding

The research was supported by the Hubei Provincial Key R&D Program (Grant number: 2022BCA034).

Declarations

Competing interests

The authors declare no competing interests.

Additional information

Supplementary Information The online version contains supplementary material available at https://doi.org/10.1038/s41598-024-84489-8.

Correspondence and requests for materials should be addressed to C.L. or L.W.